

# Intramolecular Ligand Hydroxylation: Mechanistic Studies on the Reaction of a Copper(I) Schiff Base Complex with Dioxygen<sup>†</sup>

Sara Ryan, Harry Adams, and David E. Fenton\*

Department of Chemistry, The University of Sheffield, Sheffield S3 7HF, U.K.

Michael Becker and Siegfried Schindler\*

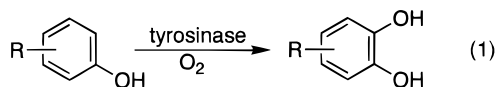
Institute for Inorganic Chemistry, University of Erlangen-Nürnberg,  
Egerlandstrasse 1, 91058 Erlangen, Germany

Received August 13, 1997

The dinuclear copper(I) complex of 1,3-bis[*N*-(2-pyridylethyl)formimidoyl]benzene, [Cu<sub>2</sub>(H-BPB-H)(CH<sub>3</sub>CN)<sub>2</sub>](BF<sub>4</sub>)<sub>2</sub>, as well as the 5-nitro derivative, [Cu<sub>2</sub>(NO<sub>2</sub>-BPB-H)(CH<sub>3</sub>CN)<sub>2</sub>](BF<sub>4</sub>)<sub>2</sub>, react with dioxygen to form phenolate-bridged complexes as products. In a detailed kinetic study activation parameters of  $\Delta H^\ddagger = 47 \pm 9$  kJ/mol,  $\Delta S^\ddagger = -53 \pm 11$  J/(mol K), and  $\Delta V^\ddagger = -9.5 \pm 0.5$  cm<sup>3</sup>/mol for the reaction of [Cu<sub>2</sub>(H-BPB-H)(CH<sub>3</sub>CN)<sub>2</sub>](BF<sub>4</sub>)<sub>2</sub> with dioxygen were obtained which account, together with further kinetic findings, for the occurrence of an intermediate peroxo complex that cannot be observed spectroscopically. The crystal structures of the products of the reaction were determined. Crystal data: complex [Cu<sub>2</sub>(H-BPB-O)-OH(H<sub>2</sub>O)](BF<sub>4</sub>)<sub>2</sub>, formula C<sub>22</sub>H<sub>24</sub>B<sub>2</sub>-Cu<sub>2</sub>F<sub>8</sub>N<sub>4</sub>O<sub>3</sub>, monoclinic space group *P*2<sub>1</sub>/*c*, *Z* = 4, *a* = 10.122(2) Å, *b* = 28.711(6) Å, *c* = 9.283(2) Å,  $\alpha = 90^\circ$ ,  $\beta = 100.78(3)^\circ$ , and  $\gamma = 90^\circ$ ; complex [Cu<sub>2</sub>(NO<sub>2</sub>-BPB-O)-OH(H<sub>2</sub>O)<sub>3</sub>](BF<sub>4</sub>)<sub>2</sub>, formula C<sub>22</sub>H<sub>27</sub>B<sub>2</sub>Cu<sub>2</sub>F<sub>8</sub>N<sub>5</sub>O<sub>7</sub>, triclinic space group, *P*1̄, *Z* = 2, *a* = 10.144(2) Å, *b* = 10.7612(2) Å, and *c* = 16.000(4) Å.

## Introduction

A dinuclear copper center forms the active site of the enzyme tyrosinase, a monooxygenase responsible for the hydroxylation of a substrate as shown in eq 1.<sup>1,2</sup>



This reaction was first modeled successfully by Karlin and co-workers, who found that an intramolecular ligand hydroxylation occurred during the reaction of [Cu<sub>2</sub>(XYL-H)]<sup>2+</sup> with dioxygen (Figure 1).<sup>3,4</sup> The peroxo complex [Cu<sub>2</sub>(XYL-H)-O<sub>2</sub>]<sup>2+</sup> could not be isolated, but its occurrence as an intermediate during this reaction was proved spectroscopically in a detailed kinetic study.<sup>5,6</sup> Interestingly this reaction was not observed when pyridine was replaced by pyrazole or benzimidazole, but in some cases substrate hydroxylation was successfully demonstrated.<sup>7–10</sup>

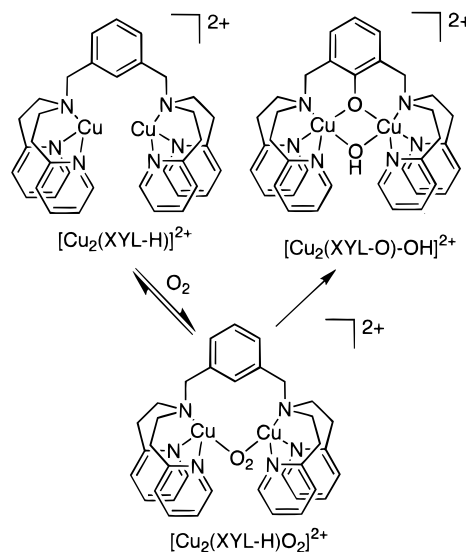


**Figure 1.** Intramolecular hydroxylation during the reaction of [Cu<sub>2</sub>(XYL-H)]<sup>2+</sup> with dioxygen.<sup>5</sup>

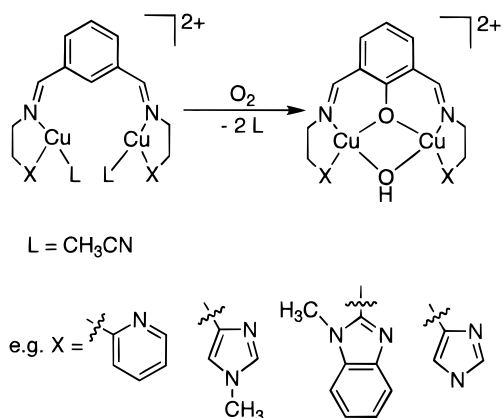
In contrast to these findings it was found that intramolecular hydroxylation depends much less critically on the ligands employed if dinuclear copper(I) Schiff base complexes are used (Scheme 1).<sup>11–17</sup> So far there is limited knowledge on the

<sup>†</sup> This paper is dedicated to Prof. Horst Elias on the occasion of his 65th birthday.

- (1) Lerch, K. *ACS Symp. Ser.* **1995**, 600, 64.
- (2) Sánchez-Ferrer, A.; Rodríguez-López, J. N.; García-Cánovas, F.; García-Carmona, F. *Biochim. Biophys. Acta* **1995**, 1247, 1.
- (3) Karlin, K. D.; Dahlstrom, P. L.; Cozzette, S. N.; Scensny, P. M.; Zubieta, J. *J. Chem. Soc., Chem. Commun.* **1981**, 881.
- (4) Karlin, K. D.; Hayes, J. C.; Gultneh, Y.; Cruse, R. W.; McKown, J. W.; Hutchinson, J. P.; Zubieta, J. *J. Am. Chem. Soc.* **1984**, 106, 2121.
- (5) Karlin, K. D.; Nasir, M. S.; Cohen, B. I.; Cruse, R. W.; Kaderli, S.; Zuberbühler, A. D. *J. Am. Chem. Soc.* **1994**, 116, 1324.
- (6) Cruse, R. W.; Kaderli, S.; Karlin, K. D.; Zuberbühler, A. D. *J. Am. Chem. Soc.* **1988**, 110, 6882.
- (7) Sorrell, T. N.; Vankai, V. A.; Garrity, M. L. *Inorg. Chem.* **1991**, 30, 207.
- (8) Sorrell, T. N.; Garrity, M. L. *Inorg. Chem.* **1991**, 30, 210.

- (9) Casella, L.; Gullotti, M.; Radaelli, R.; Di Gennaro, P. *J. Chem. Soc., Chem. Commun.* **1991**, 1611.
- (10) Sorrell, T. N.; Malachowski, M. R.; Jameson, D. L. *Inorg. Chem.* **1982**, 21, 1, 3250.
- (11) Drew, M. G. B.; Trocha-Grimshaw, J.; McKillop, K. P. *Polyhedron* **1989**, 8, 2513.
- (12) Casella, L.; Rigoni, L. *J. Chem. Soc., Chem. Commun.* **1985**, 1668.

## Scheme 1



mechanism of these reactions<sup>5</sup> that could provide better understanding of monooxygenase activity and furthermore help in the development of homogeneous catalysis for selective oxidations.<sup>18,19</sup> Here we present a mechanistic study on the reaction of the dinuclear copper complexes of 1,3-bis[*N*-(2-pyridylethyl)formimidoyl]benzene, [Cu<sub>2</sub>(H-BPB-H)(CH<sub>3</sub>CN)<sub>2</sub>](BF<sub>4</sub>)<sub>2</sub> (**1**), and its 5-nitro derivative, [Cu<sub>2</sub>(NO<sub>2</sub>-BPB-H)(CH<sub>3</sub>CN)<sub>2</sub>](BF<sub>4</sub>)<sub>2</sub> (**2**), with dioxygen, reactions first reported by Feringa and co-workers.<sup>16,20</sup>

## Experimental Section

**Materials and Methods.** Reagents and solvents used were of commercially available reagent quality. UV-vis spectra were measured on a Hewlett-Packard 8452 A spectrophotometer. <sup>1</sup>H NMR spectra were recorded on either a Bruker ACF-250 or Bruker DXP 300 Avance spectrometer. Elemental analyses were carried out by the University of Sheffield microanalytical services. Infrared spectra were recorded as KBr disks or as liquid films between NaCl plates, using a Perkin-Elmer 1600 infrared spectrophotometer (4000–400 cm<sup>-1</sup>). Electron impact (EI) and chemical impact (CI, ammonia) mass spectra were recorded with a Kratos MS25 instrument. Positive ion fast atom bombardment (FAB) mass spectra were recorded using a Kratos MS80 or a VG Prospec spectrometer. (The matrix used was 4-nitrobenzyl alcohol or glycerol.) [Cu(CH<sub>3</sub>CN)<sub>4</sub>](BF<sub>4</sub>)<sub>2</sub><sup>21</sup> and **1**<sup>16</sup> were synthesized according to literature methods.

**5-Nitroisophthalaldehyde.** The dialdehyde was prepared by following a modified literature procedure.<sup>22</sup> A mixture of ammonium sulfate (4 g), concentrated sulfuric acid (2 g), and nitric acid (2 g) was cooled to -50 °C, and a solution of isophthalaldehyde (1 g) in concentrated sulfuric acid (12 g) was added. The mixture attained room temperature during 12 h and was kept at this temperature for a further 12 h. The mixture was poured onto ice, filtered, and washed with water. Recrystallization from diethyl ether gave 5-nitroisophthalaldehyde in a 60% yield. <sup>1</sup>H NMR (CD<sub>3</sub>CN): δ 10.15 (s, 2H, CHO), 8.9 (d, 2H, ArH), 8.7 (s, 1H, ArH). Anal. Calcd for C<sub>8</sub>H<sub>5</sub>NO<sub>4</sub>: C, 53.64; H, 2.81;

N, 7.82. Found: C, 53.07; H, 2.61; N, 7.55. IR (KBr): 1698 (s, ν<sub>CO</sub>), 1538, 1360 cm<sup>-1</sup> (m, ν<sub>NO<sub>2</sub></sub>).

**1,3-Bis[*N*-(2-pyridylethyl)formylimido]-5-nitrobenzene.** A mixture of 5-nitroisophthalaldehyde (0.9 g, 5 mmol) and (2-(2-pyridyl)ethyl)amine (1.22 g, 10 mmol) in CH<sub>2</sub>Cl<sub>2</sub> (50 mL) was stirred for 1 h. Next, Na<sub>2</sub>SO<sub>4</sub> (1 g) was added and the solution stirred for 1/2 h. Filtration and removal of solvent in vacuo gave a yellow oil. Yield: 70%. <sup>1</sup>H NMR (CDCl<sub>3</sub>): δ 3.15 (t, 4H), 4.04 (t, 4H), 7.15 (m, 4H), 7.53 (t, 4H), 8.19 (m, 3H), 8.48 (m, 4H). <sup>13</sup>C NMR (CDCl<sub>3</sub>): 39.26, 60.95, 121.44, 123.71, 123.94, 132.62, 136.32, 138.20, 149.43, 158.66, 159.40. MS (EI<sup>+</sup>) (*m/e*): P<sup>+</sup>, 387 (28%). Anal. Calcd for C<sub>22</sub>H<sub>21</sub>N<sub>5</sub>O<sub>2</sub>: C, 65.15; H, 5.72; N, 17.27. Found: C, 65.93; H, 5.67; N, 17.65. IR (NaCl): 1534, 1347 cm<sup>-1</sup> (ν<sub>NO<sub>2</sub></sub>), 1647 (ν<sub>CN</sub>).

[Cu<sub>2</sub>(NO<sub>2</sub>-BPB-H)(CH<sub>3</sub>CN)<sub>2</sub>](BF<sub>4</sub>)<sub>2</sub> (**2**). The complex was prepared as a solid in the same way as **1**.<sup>16</sup> Yield: 90%. Anal. Calcd for **2** (Cu<sub>2</sub>C<sub>26</sub>H<sub>27</sub>N<sub>7</sub>O<sub>2</sub>B<sub>2</sub>F<sub>8</sub>)·1/2[Cu(CH<sub>3</sub>CN)<sub>4</sub>](BF<sub>4</sub>): C, 38.85; H, 3.59; N, 13.59. Found: C, 38.62; H, 3.83; N, 13.67. IR (KBr): 2225 (m, ν<sub>CN</sub>), 1625, 1609 (s, ν<sub>CN</sub>), 1534, 1342 (m, ν<sub>NO<sub>2</sub></sub>), 1060 cm<sup>-1</sup> (br, ν<sub>BF</sub>). No crystals suitable for structural characterization were obtained. For the kinetic measurements the complex was prepared in situ by adding [Cu(CH<sub>3</sub>CN)<sub>4</sub>](BF<sub>4</sub>) to a solution of 1,3-bis[*N*-(2-pyridylethyl)formylimido]-5-nitrobenzene in acetone under nitrogen.

[Cu<sub>2</sub>(H-BPB-O)OH(H<sub>2</sub>O)](BF<sub>4</sub>)<sub>2</sub> (**3'**) and [Cu<sub>2</sub>(NO<sub>2</sub>-BPB-O)OH(H<sub>2</sub>O)<sub>3</sub>](BF<sub>4</sub>)<sub>2</sub> (**4**). The complexes were obtained by oxidizing the copper(I) complexes in dichloromethane/methanol solution (10:1) in a reaction vessel open to air while stirred for 3 h. The crude complexes, obtained by evaporation from the reaction mixture, were recrystallized from ethanol/water (1:1) mixtures. Yields: 80%. Crystals suitable for X-ray analysis were obtained. Anal. Calcd for **4** (bulk sample recrystallization) (Cu<sub>2</sub>C<sub>22</sub>H<sub>21</sub>N<sub>5</sub>O<sub>4</sub>B<sub>2</sub>F<sub>8</sub>): C, 36.69; H, 2.94; N, 9.72. Found: C, 36.72; H, 2.96; N, 9.44. IR (KBr): 3567 (m, ν<sub>OH</sub>), 1646 (s, ν<sub>CN</sub>), 1585, 1339 (m, ν<sub>NO<sub>2</sub></sub>), 1000–1080 cm<sup>-1</sup> (br, ν<sub>BF</sub>).

**Single-Crystal X-ray Structure Determinations.** Crystal data and experimental conditions for complexes **3'** and **4** are listed in Table 1. The molecular structures are illustrated in Figures 2 and 3, respectively. Selected bond lengths and bond angles with standard deviations in parentheses are presented in Table 2. Three-dimensional, room-temperature X-ray data were collected in the range 3.5 < 2θ < 45° on a Siemens P4 diffractometer by the ω-scan method. The collected reflections were corrected for Lorentz and polarization effects (but not for absorption). The structures were solved by direct methods and refined by full-matrix least-squares methods on F<sup>2</sup>. Hydrogen atoms were included in calculated positions and refined in riding mode. For **3'** a weighting scheme w = 1/[σ<sup>2</sup>(F<sub>o</sub><sup>2</sup>) + (0.0923P)<sup>2</sup> + 8.5520P] (w = 1/[σ<sup>2</sup>(F<sub>o</sub><sup>2</sup>) + (0.0625P)<sup>2</sup> + 5.8035P] for **4**), where P = (F<sub>o</sub><sup>2</sup> + 2F<sub>c</sub><sup>2</sup>)/3, was used in the latter stages of refinement. Complex scattering factors were taken from the program package SHELXL93<sup>23</sup> as implemented on the Viglen 486dx computer.

**Kinetic Measurements.** Reagent quality acetone either was used directly or was dried over Drierite (Aldrich) and immediately after distillation transferred into a glovebox (Braun, Garching, Germany (dioxygen and water content less than 1 ppm)). Solutions of complexes for the kinetic measurements were prepared in the glovebox and transferred with gastight syringes to the stopped-flow instrument. A dioxygen saturated solution was prepared bubbling dioxygen through acetone in a syringe (solubility of dioxygen in acetone = 0.0102 M<sup>24</sup>). Dilution was accomplished by mixing the solution with argon-saturated acetone. The reaction was studied under pseudo-first-order conditions, and time-resolved spectra were recorded on an Applied Photophysics stopped-flow SX.18MV (Leatherhead, U.K.) equipped with a J&M TIDAS 16-500 diode array spectrophotometer (J&M, Aalen, Germany). Data fitting was carried out using the integrated J&M software Kinspec or the program Specfit (Spectrum Software Associates, Chapel Hill, NC). The effect of pressure was measured on a homemade high-pressure stopped flow instrument described elsewhere.<sup>25</sup>

(13) Casella, L.; Gullotti, M.; Pallanza, G. *Biochem. Soc. Trans.* **1988**, *16*, 821.

(14) Casella, L.; Gullotti, M.; Pallanza, G.; Rigoni, L. *J. Am. Chem. Soc.* **1988**, *110*, 4221.

(15) Casella, L.; Gullotti, M.; Bartosek, M.; Pallanza, G.; Laurenti, E. *J. Chem. Soc., Chem. Commun.* **1991**, 1235.

(16) Gelling, O. J.; van Bolhuis, F.; Meetsma, A.; Feringa, B. L. *J. Chem. Soc., Chem. Commun.* **1988**, 552.

(17) Menif, R.; Martell, A. E.; Squattrito, P. J.; Clearfield, A. *Inorg. Chem.* **1990**, *29*, 9, 4723.

(18) Reedijk, J. In *Bioinorganic Catalysis*; Reedijk, J., Ed.; Marcel Dekker: New York, 1993.

(19) Thorp, H. H.; Pecoraro, V. L. *Mechanistic Bioinorganic Chemistry*; American Chemical Society: Washington, DC, 1995.

(20) Feringa, B. L. In *Bioinorganic Chemistry of Copper*; Karlin, K. D., Tyeklár, Z., Eds.; Chapman & Hall: New York, 1993.

(21) Kubas, G. J. *Inorg. Synth.* **1979**, 1990.

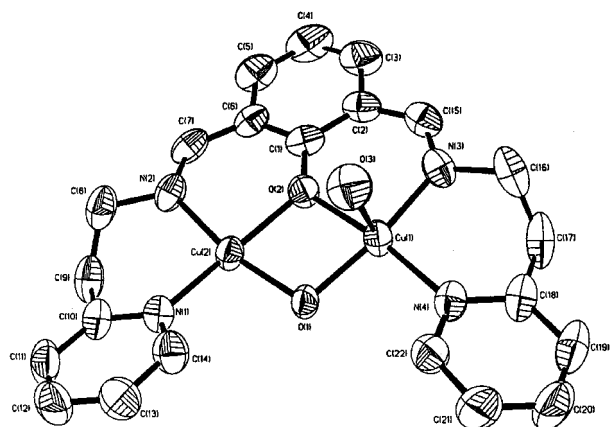
(22) Jenkins, K. F. *J. Chem. Soc.* **1957**, 1172.

(23) Sheldrick, G. M. SHELXL93, An integrated system for solving and refining crystal structures from diffraction data, University of Göttingen, Germany, 1993.

(24) Lühring, P.; Schumpe, A. *J. Chem. Eng. Data* **1989**, *34*, 250.

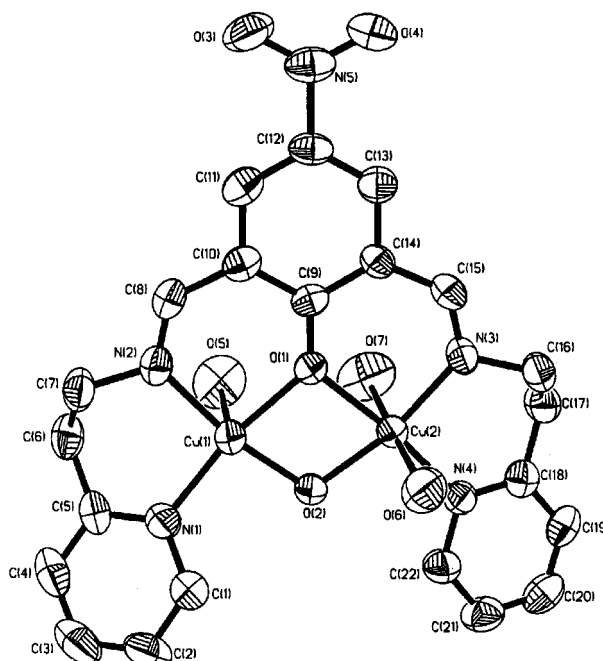
**Table 1.** Crystal and Structure Refinement Data for **3'** and **4**

empirical formula	C <sub>22</sub> H <sub>24</sub> B <sub>2</sub> Cu <sub>2</sub> F <sub>8</sub> N <sub>4</sub> O <sub>3</sub>	C <sub>22</sub> H <sub>27</sub> B <sub>2</sub> Cu <sub>2</sub> F <sub>8</sub> N <sub>5</sub> O <sub>7</sub>
fw	693.15	774.19
temp (K)	293(2)	293(2)
wavelength (Å)	0.710 73	0.710 73
cryst system	monoclinic	triclinic
space group	<i>P</i> 2 <sub>1</sub> / <i>c</i>	<i>P</i> 1
<i>a</i> (Å)	10.122(2)	10.144(2)
<i>b</i> (Å)	28.711(6)	10.761(2)
<i>c</i> (Å)	9.283(2)	16.000(4)
α (deg)	90	106.15(2)
β (deg)	100.78(3)	96.13(2)
γ (deg)	90	114.810(10)
<i>V</i> (Å <sup>3</sup> )	2650.1(10)	1479.6(5)
<i>Z</i>	4	2
<i>D</i> (calcd) (Mg/m <sup>3</sup> )	1.737	1.738
abs coeff (mm <sup>-1</sup> )	1.695	1.538
<i>F</i> (000)	1392	780
cryst size (mm)	0.64 × 0.35 × 0.17	0.55 × 0.34 × 0.22
θ range for data collcn (deg)	2.05–22.52	2.17–22.50
index ranges	−10 ≤ <i>h</i> ≤ 10, −30 ≤ <i>k</i> ≤ 1, −1 ≤ <i>l</i> ≤ 9	−1 ≤ <i>h</i> ≤ 10, −1 0 ≤ <i>k</i> ≤ 10, −17 ≤ <i>l</i> ≤ 17
reflens colld	4403	4534
indepdt reflens	3455 ( <i>R</i> <sub>int</sub> = 0.0634)	3757 ( <i>R</i> <sub>int</sub> = 0.0265)
refinement method	full-matrix least squares on <i>F</i> <sup>2</sup>	full-matrix least squares on <i>F</i> <sup>2</sup>
data/restraints/params	3453/24/370	3757/30/424
goodness of fit on <i>F</i> <sup>2</sup>	1.050	1.044
final <i>R</i> indices [ <i>I</i> > σ( <i>I</i> )]	<i>R</i> 1 = 0.0641, w <i>R</i> 2 = 0.1617	<i>R</i> 1 = 0.0585, w <i>R</i> 2 = 0.1403
<i>R</i> indices (all data)	<i>R</i> 1 = 0.0868, w <i>R</i> 2 = 0.1821	<i>R</i> 1 = 0.0840, w <i>R</i> 2 = 0.1578
largest diff peak and hole (e Å <sup>-3</sup> )	1.254 and −0.807	0.761 and −0.588

**Figure 2.** ORTEP view of the cation of **3'**. The thermal ellipsoids are at the 50% probability level, and the hydrogen atoms are omitted for clarity.

## Results and Discussion

While it seems to be very likely for the copper(I) complexes in Scheme 1 to undergo a similar reaction pathway as was shown for [Cu<sub>2</sub>(XYL-H)]<sup>2+</sup> (Figure 1), so far there is no solid proof for occurrence of a copper(II) peroxo Schiff base complex as an intermediate. In addition to the complexes in Scheme 1 it was shown that intramolecular hydroxylation also occurred during the reaction of dioxygen with a macrocyclic copper(I) Schiff base complex [Cu<sub>2</sub>(mac)(CH<sub>3</sub>CN)<sub>2</sub>]<sup>2+</sup> and a peroxo intermediate was postulated but not detected spectroscopically.<sup>17,26</sup> To gain more understanding on the reactions of copper(I) Schiff base complexes with dioxygen, we therefore decided to study the reaction of **1** with dioxygen. This complex is similar to [Cu<sub>2</sub>(XYL-H)]<sup>2+</sup> (Figure 1) missing two of the pyridine arms and possessing imine nitrogens instead of amines. Because of this similarity, we hoped it would be more likely to

**Figure 3.** ORTEP view of the cation of **4**. The thermal ellipsoids are at the 50% probability level, and the hydrogen atoms are omitted for clarity.

observe a peroxo intermediate spectroscopically during the kinetic investigation. Furthermore, we prepared **2**, the 5-nitro derivative of **1**, for investigations because Feringa and co-workers claimed observation of reversible dioxygen binding to this complex but did not give further details.<sup>27</sup>

**Structures.** Before initiating the kinetic study, we investigated the reactions of **1** and **2** with dioxygen on a synthetic scale and were able to obtain crystals suitable for X-ray study of the product complexes **3'** and **4**. The structure of **3'** has a water molecule coordinated to one of the copper ions and is

(25) van Eldik, R.; Gaede, W.; Wieland, S.; Kraft, J.; Spitzer, M.; Palmer, D. A. *Sci. Instrum.* **1993**, *64*, 1355.

(26) Menif, R.; Martell, A. E. *J. Chem. Soc., Chem. Commun.* **1989**, 1521.

(27) Gelling, O. J.; Feringa, B. E. *J. Am. Chem. Soc.* **1990**, *112*, 7599.

**Table 2.** Selected Bond Lengths and Bond Angles with Standard Deviations in Parentheses for Complexes **3'** and **4**

Bond Lengths (Å) for <b>3'</b>			
Cu(1)–O(1)	1.908(5)	Cu(2)–O(1)	1.894(5)
Cu(1)–O(2)	1.982(5)	Cu(2)–O(2)	1.974(5)
Cu(1)–O(3)	2.335(6)	Cu(2)–N(2)	1.954(6)
Cu(1)–N(3)	1.940(7)	Cu(2)–N(1)	1.996(7)
Cu(1)–N(4)	1.999(7)	Cu(1)–Cu(2)	3.0294(14)
Bond Angles (deg) for <b>3'</b>			
O(1)–Cu(1)–N(3)	164.6(3)	O(1)–Cu(1)–O(2)	76.3(2)
N(3)–Cu(1)–O(2)	90.7(3)	O(1)–Cu(1)–N(4)	96.0(3)
N(3)–Cu(1)–N(3)	96.4(3)	O(2)–Cu(1)–N(4)	171.8(3)
O(1)–Cu(1)–O(3)	94.1(2)	N(3)–Cu(1)–O(3)	94.8(3)
O(2)–Cu(1)–O(3)	92.1(2)	N(4)–Cu(1)–O(3)	91.2(3)
O(1)–Cu(1)–Cu(2)	37.0(2)	N(3)–Cu(1)–Cu(2)	130.7(2)
O(2)–Cu(1)–Cu(2)	39.9(2)	N(4)–Cu(1)–Cu(2)	132.7(2)
O(3)–Cu(1)–Cu(2)	88.7(2)	O(1)–Cu(2)–N(2)	168.3(3)
O(1)–Cu(2)–O(2)	76.8(2)	N(2)–Cu(2)–O(2)	91.5(3)
O(1)–Cu(2)–N(1)	95.3(2)	N(2)–Cu(2)–N(1)	96.3(3)
O(2)–Cu(2)–N(1)	162.9(2)	O(1)–Cu(2)–Cu(1)	37.3(2)
N(1)–Cu(2)–Cu(1)	131.3(2)	O(2)–Cu(2)–Cu(1)	40.12(14)
N(1)–Cu(2)–Cu(1)	128.6(2)		
Bond Lengths (Å) for <b>4</b>			
Cu(1)–O(1)	1.982(5)	Cu(2)–O(1)	2.019(4)
Cu(1)–O(2)	1.919(5)	Cu(2)–O(2)	1.913(5)
Cu(1)–O(5)	2.486(7)	Cu(2)–O(6)	2.430(6)
Cu(1)–N(1)	1.994(6)	Cu(2)–O(7)	2.661(8)
Cu(1)–N(2)	1.957(6)	Cu(2)–N(3)	1.949(6)
Cu(1)–Cu(2)	3.0309(14)	Cu(2)–N(4)	2.013(6)
Bond Angles (deg) for <b>4</b>			
O(2)–Cu(1)–N(2)	169.7(2)	O(2)–Cu(1)–O(1)	78.7(2)
N(2)–Cu(1)–O(1)	91.9(2)	O(2)–Cu(1)–N(1)	94.2(2)
N(2)–Cu(1)–N(1)	95.8(2)	O(1)–Cu(1)–N(1)	166.4(2)
O(2)–Cu(1)–O(5)	88.4(2)	N(2)–Cu(1)–O(5)	87.2(2)
O(1)–Cu(1)–O(5)	89.0(2)	N(1)–Cu(1)–O(5)	102.6(2)
O(2)–Cu(1)–Cu(2)	37.66(14)	N(2)–Cu(1)–Cu(2)	133.0(2)
O(1)–Cu(1)–Cu(2)	41.20(13)	N(1)–Cu(1)–Cu(2)	130.2(2)
O(5)–Cu(1)–Cu(2)	90.6(2)	O(2)–Cu(2)–N(3)	168.2(2)
O(2)–Cu(2)–N(4)	95.0(2)	N(3)–Cu(2)–N(4)	96.5(2)
O(2)–Cu(2)–O(1)	78.0(2)	N(3)–Cu(2)–O(1)	90.4(2)
N(4)–Cu(2)–O(1)	172.3(2)	O(2)–Cu(2)–O(6)	95.6(2)
N(3)–Cu(2)–O(6)	87.0(2)	N(4)–Cu(2)–O(6)	89.2(2)
O(1)–Cu(2)–O(6)	94.6(2)	O(2)–Cu(2)–O(7)	85.5(3)
N(3)–Cu(2)–O(7)	92.4(3)	N(4)–Cu(2)–O(7)	88.6(2)
O(1)–Cu(2)–O(7)	87.7(2)	O(6)–Cu(2)–O(7)	177.6(2)
O(2)–Cu(2)–Cu(1)	37.8(2)	N(3)–Cu(2)–Cu(1)	130.6(2)
N(4)–Cu(2)–Cu(1)	132.8(2)	O(1)–Cu(2)–Cu(1)	40.28(13)
O(6)–Cu(2)–Cu(1)	94.35(14)	O(7)–Cu(2)–Cu(1)	87.8(2)

therefore different from the structure of  $[\text{Cu}_2(\text{H-BPB-O})\text{OH}](\text{BF}_4)_2$  (**3**) reported previously.<sup>16</sup> In **3** each Cu(II) ion is in a slightly distorted square planar  $[\text{N}_2\text{O}_2]$  coordination environment provided by the ligand and exogenous hydroxo bridge. The structures of **3'** and **4** confirm incorporation of two oxygen atoms into the complex with one oxygen atom being inserted into an aryl-hydrogen bond (*arene hydroxylation*) and the second being incorporated into the hydroxo bridge.

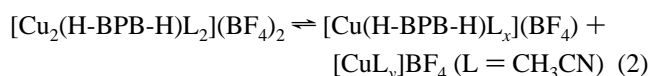
Interestingly both dicopper(II) complexes exhibited coordination number asymmetry<sup>28</sup> caused by further complexation by water molecules. In **3'**, Figure 2, Cu(1) is five coordinate and Cu(2) is four coordinate while in **4**, Figure 3, Cu(1) is five coordinate and Cu(2) is six coordinate. The absence of any intermolecular hydrogen bonding between the nitro groups of **4** and the coordinated water molecules on adjacent complex molecules suggests that it is likely that the electronic effect of the nitro group is responsible for the enhanced coordination at the dinuclear copper center in that molecule. The bridges in the  $\text{Cu}_2\text{O}_2$  units are essentially symmetric, and the  $\text{Cu}_2\text{O}_2$  units are less deviated from planarity ( $5.9$  and  $1^\circ$ ) than in the nonsolvated complex ( $9.3^\circ$ ). The Cu(II)–Cu(II) separations are

$3.029$  and  $3.031$  Å, respectively, and these are in accord with values previously obtained for dinuclear copper(II) complexes containing two symmetric single atom bridges.<sup>29</sup>

**Kinetic Measurements.** We chose the reaction of **1** with dioxygen for a detailed kinetic study because this is the only case of binuclear copper Schiff base complexes according to Scheme 1 where the crystal structure of the reactant and the product are known. Because of the similarity of **1** to  $[\text{Cu}_2(\text{XYL-H})]^{2+}$ , it seemed more than likely to observe the postulated peroxo intermediate spectroscopically. Furthermore, it was claimed that **2**, the 5-nitro derivative of **1**, formed a peroxo complex.<sup>27</sup> Our first kinetic measurements of the reaction of **1** with dioxygen were performed in methanol so that we would be able to compare the results with our recent work on the complex  $[\text{Cu}_2(\text{mac})(\text{CH}_3\text{CN})_2](\text{PF}_6)_2$ .<sup>30</sup> Unfortunately, in this solvent several reaction steps were observed and an acceptable fitting of the absorbance–time traces was not possible. Therefore, we used acetone, which in general seems to be a good solvent for such measurements.<sup>31</sup> Our first finding, in contrast to our earlier mechanistic studies of the macrocyclic complex  $[\text{Cu}_2(\text{mac})(\text{CH}_3\text{CN})_2](\text{PF}_6)_2$ , was the observation of two reaction steps, both dependent on the dioxygen concentration. This seemed rather strange because it meant most likely a parallel reaction which should not occur if the reaction would proceed quantitatively from **1** to the hydroxylated product.

It is known from the work of Feringa and co-workers that for the 1-methoxy derivative of **1** several species can exist in solution which differ by the number of coordinated acetonitrile molecules.<sup>27</sup> Complexes with no, two, or four molecules of acetonitrile were described. Furthermore, it was found that a mononuclear copper(I) polymer complex formed together with starting material  $[\text{Cu}(\text{CH}_3\text{CN})_4](\text{BF}_4)$ .<sup>27</sup> Similar behavior for related complexes was discussed by Casella et al.,<sup>14</sup> and we also observed the same problems during the synthesis or recrystallization of **1** and **2**. These findings indicate that several species exist in the solutions used in our kinetic measurements.

In our efforts to simplify the kinetic behavior, an excess of  $[\text{Cu}(\text{CH}_3\text{CN})_4](\text{BF}_4)$  was added to the complex solution resulting in the effect that the slower reaction step gained in amplitude while the amplitude of the faster step nearly disappeared. This indicated an equilibrium between **1** and a mononuclear complex/ $[\text{Cu}(\text{CH}_3\text{CN})_y]\text{BF}_4$  mixture in solution (eq 2,  $L = \text{CH}_3\text{CN}$ ).



While we do not know exactly the nature of the compounds on the right side in eq 2, we could force the equilibrium to the left side by adding an excess of  $[\text{Cu}(\text{CH}_3\text{CN})_4](\text{BF}_4)$  to the solution.  $^1\text{H}$  NMR work further supported these findings. The  $^1\text{H}$  NMR of **1** in acetone- $d_6$  shown in Figure 4a is broad because of the occurrence of a fast equilibrium process between two species. Addition of  $[\text{Cu}(\text{CH}_3\text{CN})_4](\text{BF}_4)$  to an NMR sample of **1** in acetone- $d_6$  gave sharp signals as shown in Figure 4b. This indicated again that under these conditions the equilibrium in eq 2 is forced to the left side. Lowering the temperature of a sample of **1** in acetone- $d_6$  did lead to sharp  $^1\text{H}$  NMR signals at 213 K and clearly showed the occurrence of at least two species (Figure 4c). Increasing the temperature resulted again in the

(29) Satcher, J. H.; Droege, M. W.; Weakley, T. J. R.; Taylor, R. T. *Inorg. Chem.* **1995**, *34*, 3317.

(30) Becker, M.; Schindler, S.; van Eldik, R. *Inorg. Chem.* **1994**, *33*, 5370.

(31) Becker, M.; Schindler, S. Unpublished results.

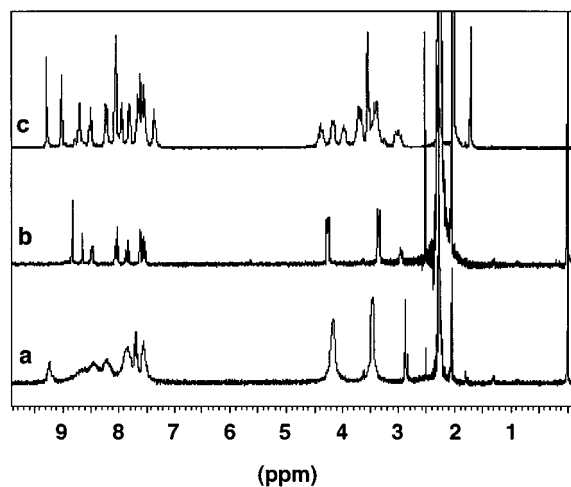


**Figure 4.** (a)  $^1\text{H}$  NMR of **1** in acetone- $d_6$  at 25 °C. (b)  $^1\text{H}$  NMR of **1** in acetone- $d_6$  with an 10-fold excess of  $[\text{Cu}(\text{CH}_3\text{CN})_4](\text{BF}_4)$  at 25 °C. (c)  $^1\text{H}$  NMR of **1** in acetone- $d_6$  at -60 °C.

broad  $^1\text{H}$  NMR signals shown in Figure 4a. These findings are in contrast to NMR studies on  $[\text{Cu}_2(\text{XYL-H})](\text{PF}_6)_2$ , where we only could observe sharp signals over the whole temperature range.<sup>31</sup>

Even though we were able to suppress one reaction step by adding  $[\text{Cu}(\text{CH}_3\text{CN})_4](\text{BF}_4)$  to solutions of the complex used in the kinetic measurements as discussed above, we were not successful in fitting our observed absorbance–time traces to a simple mathematical function. Instead of a single exponential absorbance time trace we obtained traces which obviously included a linear part in the beginning of the reaction. This is typical for many catalyzed reactions as discussed for example by Espenson,<sup>32</sup> but none of these data treatments allowed us to obtain an acceptable fit of our data. Therefore, we abandoned this approach of adding a 2–10-fold excess of  $[\text{Cu}(\text{CH}_3\text{CN})_4](\text{BF}_4)$  to the solutions used in our kinetic measurements.

We did fit our data to the sum of two exponential functions as described above, but with the results of the additional NMR experiments we now could assign the slower step ( $k_{\text{obs}2}$ ) to the reaction of the dinuclear complex **1** with dioxygen, the reaction we actually wanted to study.

The spectral changes that occurred during that reaction under these conditions are shown in Figure 5, and the insert shows the data fit to the sum of two exponential functions at 360 nm. The buildup of an absorbance maxima at 360 nm indicates the formation of the product, the phenolate-bridged complex **3**, but at nearly the same wavelength charge-transfer bands of Cu–OH are also observed. This can be shown independently of the kinetic measurements, by adding small amounts of sodium hydroxide dissolved in methanol to a solution of the ligand together with a stoichiometric amount of copper perchlorate and observing the spectral changes. A spectrum quite similar to that of the phenolate-bridged species was obtained, a finding comparable with spectroscopic titrations already performed with a different series of complexes.<sup>33</sup> This emphasizes the importance of verifying intramolecular ligand hydroxylation by means other than UV–vis spectroscopy. Furthermore, we obtained a spectrum with an absorbance maximum at  $\sim 370$  nm (Figure 6) with a mononuclear copper(II) complex obtained from the oxidation of a copper(I) complex with the ligand derived from

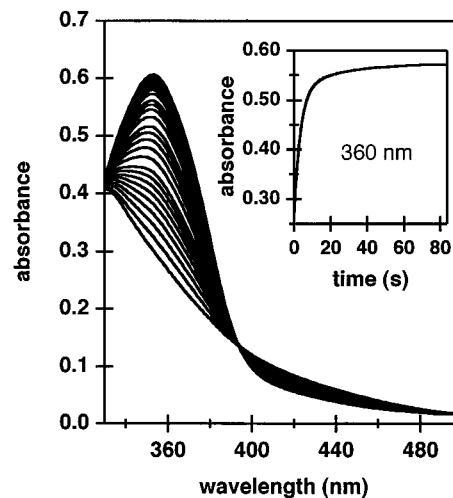


**Figure 5.** Spectral changes during the reaction of **1** with dioxygen in acetone ( $T = 25.0$  °C,  $[\text{complex}] = 0.1$  mM,  $[\text{O}_2] = 1.787$  mM).

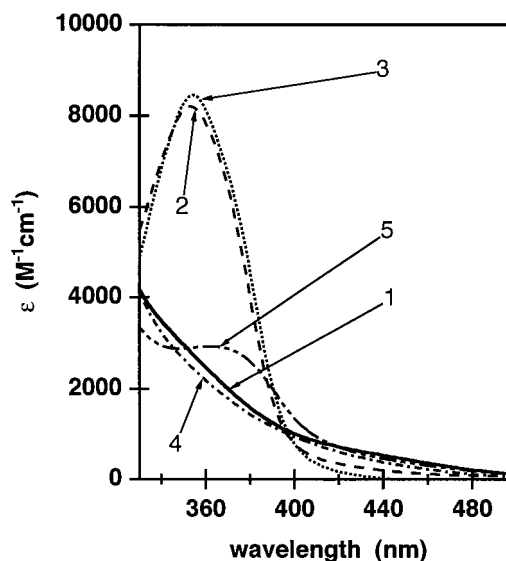


**Figure 6.** UV–vis spectra of different copper species as explained in the text ( $T = 25.0$  °C, solvent = acetone): (1)  $[\text{Cu}_2(\text{H-BPB-H})(\text{CH}_3\text{CN})_2](\text{BF}_4)_2$ ; (2) oxidized  $[\text{Cu}_2(\text{H-BPB-H})(\text{CH}_3\text{CN})_2](\text{BF}_4)_2$ ; (3)  $[\text{Cu}_2(\text{H-BPB-O-OH})(\text{BF}_4)_2]$ , isolated; (4) mononuclear Cu(I) complex; (5) oxidized mononuclear Cu(I) complex.

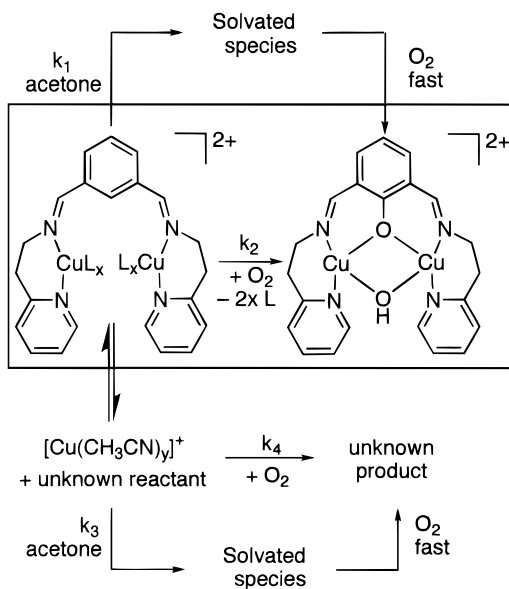
benzaldehyde and (2-(2-pyridyl)ethyl)amine (the single arm analogue of  $[\text{Cu}_2(\text{H-BPB-H})]^{2+}$ ). Therefore we are quite sure that the second product in the reaction of **1** with dioxygen is a mono- or dinuclear copper hydroxy complex with ligands derived from the complex shown on the right side in eq 2.

In that context it should further be mentioned that Casella and co-workers investigated the reaction of mononuclear copper imine complexes with dioxygen and found that in no case hydroxylation of the benzene ring occurred.<sup>20</sup> This is an indication of the necessity to have a dinuclear copper complex to observe intramolecular ligand hydroxylation and that a peroxo intermediate is likely to occur during the reaction. But—as found for  $[\text{Cu}_2(\text{mac})(\text{CH}_3\text{CN})_2](\text{PF}_6)_2$ —no peroxo intermediate could be detected during the reaction; spectral changes only show the reactant and the final product; this was also observed for other solvents (dichloromethane, methanol). Looking at the reaction at low temperatures did show the same effect as for the macrocyclic complex.<sup>31</sup> The reaction slowed to become unreactive when the temperature was lowered, but no peroxo complex was observed spectrophotometrically.

(32) Espenson, J. H. *Chemical Kinetics and Reaction Mechanisms*, 2nd ed.; McGraw-Hill: New York, 1995.

(33) Casella, L.; Carugo, O.; Gullotti, M.; Garofani, S.; Zanello, P. *Inorg. Chem.* **1993**, *32*, 2056.

## Scheme 2



Performing our kinetic measurements at room temperature and using dioxygen in excess over **1** (pseudo-first-order conditions) did lead to absorbance–time traces which could be fitted to the sum of two exponentials as discussed above (Figure 5). For both reactions a linear dependence of the observed rate constants  $k_{\text{obs}}$  vs dioxygen concentration was found with an intercept. The intercept indicates a reaction independent of dioxygen concentration. We assume that this reaction arises from the occurrence of a solvent-linked pathway for both reactions. In addition to a direct attack of dioxygen on the complex, acetone can form a solvated species of the complex. This step is rate determining, and then the solvated complex reacts in a fast step with dioxygen (leading to the observed intercept). It is very likely that a solvent reaction can occur that way, because as discussed above many different species with different amounts of acetonitrile bound to the complex are known. From all these findings we obtain the following rate law for the reaction of **1** with dioxygen (eq 3):

$$\frac{d[\text{product}]}{dt} = (k_1 + k_2[\text{O}_2])[\mathbf{1}] + (k_3 + k_4[\text{O}_2])[\text{complex}'] \quad (3)$$

$$[\text{product}] = \mathbf{3}' + [\text{unknown product}]$$

$$[\text{complex}'] = [\text{unknown reactant}]$$

$$k_{\text{obs1}} = k_3 + k_4[\text{O}_2] \quad k_{\text{obs2}} = k_1 + k_2[\text{O}_2]$$

The postulated reaction mechanism shown in Scheme 2 summarizes the overall findings. The dinuclear copper complex **1** is in an equilibrium with an unknown mononuclear copper(I) complex and  $[\text{Cu}(\text{CH}_3\text{CN})_4](\text{BF}_4)$ . Both **1** and the unknown mononuclear copper(I) complex can react with dioxygen and form either the phenolate-bridged complex **3** or an unknown product with similar spectroscopic absorbance maxima. Both complexes can react as well with the solvent acetone to solvated species, which then can react in a fast reaction with dioxygen to the products. The small differences in the UV–vis spectra between a solution of a pure sample of **3** (prepared independently from 2-hydroxyisophthalaldehyde, (2-(2-pyridyl)ethyl)amine, and copper(II) perchlorate) and the complex derived from the oxidation of the copper(I) complex with dioxygen are shown in Figure 6. The spectra are similar, but the obvious differences

**Table 3.** Observed Rate Constants for the Reaction of Dioxygen with **1** in Acetone

[O <sub>2</sub> ] (mmol/L)	T (°C)	p (Mpa)	k <sub>obs1</sub> (s <sup>-1</sup> )	k <sub>obs2</sub> (s <sup>-1</sup> )
5.106	10.0	0.1	0.173	0.098
4.085			0.172	0.088
3.319			0.167	0.08
2.553			0.130	0.064
5.106	15.0	0.1	1.33	0.233
4.085			1.35	0.2
3.319			1.241	0.176
2.553			1.17	0.159
5.106	20.0	0.1		0.37
4.085			2.161	0.254
3.319			1.954	0.221
2.553			1.91	0.202
5.106	25.0	0.1	2.807	0.308
4.085			2.39	0.257
3.319			2.038	0.215
2.553			1.75	0.194
5.106	30.0	0.1	3.8	0.471
4.085			3.225	0.393
3.319			2.73	0.344
2.553			2.45	0.286
5.106	35.0	0.1	5	0.599
4.085			4.14	0.511
3.319			3.15	0.446
2.553			2.54	0.352
5.106	40.0	0.1	6.45	0.761
4.085			4.18	0.584
3.319			3.46	0.519
2.553			2.45	0.427
5.106	25.0	10		0.614
		25		0.649
		50		0.703
		75		0.793
		100		0.854
		120		0.937

can be seen clearly and arise from the second product formed during the reaction of **1** and the unknown species (eq 2) with dioxygen. This is the reason that no clean isosbestic point is observed (Figure 5). Because we do not know exactly what kind of complexes occur on the right side in eq 2 and furthermore are more interested in the reaction of **1** with dioxygen (shown in the box), the reactions on the lower side of the scheme are ignored in the following discussion.

Additional support for this mechanism is obtained from experiments where the pseudo-first-order conditions were turned around. Using the complex in excess concentration compared to dioxygen did lead to absorbance–time traces which could be fit perfectly to a one exponential function. The rate law under these conditions is shown in eq 4. Using the complex in

$$\frac{d[\text{product}]}{dt} = k_{\text{obs}}[\text{O}_2] \quad (4)$$

$$k_{\text{obs}} = k_1 + k_2[\mathbf{1}] + k_3 + k_4[\text{complex}']$$

excess means that the concentrations of both complex species remain constant during the reaction and are included in the observed rate constant. Therefore, a single-exponential absorbance–time trace is observed. Unfortunately, under these conditions it was impossible to measure concentration dependencies because of the low solubility of the complex.

The temperature dependence of the reaction of dioxygen with **1** was measured, and the data are presented in Table 3. From an Eyring plot the activation parameters for  $k_2$  were calculated

to  $\Delta H^\ddagger = 47 \pm 9$  kJ/mol and  $\Delta S^\ddagger = -53 \pm 11$  J/(mol K). Values for the intercept ( $k_1$ ) had a large error and therefore will not be discussed. High-pressure stopped-flow measurements showed that the reaction rate was increased with an increase in pressure (Table 3), and an activation volume  $\Delta V^\ddagger = -9.5 \pm 0.5$  cm<sup>3</sup>/mol was calculated. The results support a mechanism very similar to that proposed in our study of the reaction of [Cu<sub>2</sub>(mac)(CH<sub>3</sub>CN)<sub>2</sub>](PF<sub>6</sub>)<sub>2</sub> with dioxygen.<sup>30</sup> In a rate-determining step a peroxo complex is formed as an intermediate which then reacts in a very fast reaction to give the final product. The negative  $\Delta S^\ddagger$  and  $\Delta V^\ddagger$  values support the concept of a highly structured transition state, formed as a result of the presence of the highly reactive and easily oxidizable cuprous species. The negative volume of activation must be a strong indication of Cu–O<sub>2</sub> bond formation that is accompanied by electron transfer to produce the Cu(II)–O<sub>2</sub>–Cu(II) peroxo intermediate. The formal oxidation of Cu(I) to Cu(II) and reduction of O<sub>2</sub> to O<sub>2</sub><sup>2-</sup> are expected to be accompanied by a significant volume collapse, partly due to intrinsic and solvational volume changes.<sup>34</sup> The activation parameters for the reaction of dioxygen with **1** compare well with those obtained for [Cu<sub>2</sub>(mac)(CH<sub>3</sub>CN)<sub>2</sub>](PF<sub>6</sub>)<sub>2</sub> ( $\Delta H^\ddagger = 32 \pm 2$  kJ/mol,  $\Delta S^\ddagger = -146 \pm 8$  J/(mol K), and  $\Delta V^\ddagger = -21 \pm 1$  cm<sup>3</sup>/mol). The higher values for the activation entropy and activation volume are probably caused by larger geometrical rearrangements for the macrocyclic complex compared to the open complex **1**. Even though the data for the macrocyclic complex are obtained from measurements in a different solvent (methanol instead of acetone), it is possible to compare the results directly because [Cu<sub>2</sub>(mac)(CH<sub>3</sub>CN)<sub>2</sub>](PF<sub>6</sub>)<sub>2</sub> reacts very similar in methanol and in acetone.<sup>31</sup> The copper(I) Schiff base complexes shown in Scheme 1 as well as [Cu<sub>2</sub>(mac)(CH<sub>3</sub>CN)<sub>2</sub>](PF<sub>6</sub>)<sub>2</sub> seem to react in general very similarly. A qualitative comparison of the reaction of the complexes in Scheme 1 with air in methanol did show nearly identical reaction rates.<sup>15</sup> We assume that the rate-determining step in a whole sequence of steps must be the attack of dioxygen on the first copper(I) ion being accompanied by an electron transfer step (leading formally to a copper(II) superoxo complex). This species then reacts very quickly to produce the peroxo complex and then again in a fast reaction sequence to give the product. Even the unknown complex in Scheme 2 reacts with similar rates with dioxygen supporting this reaction pathway. Therefore, it seems to be a general finding that the rate-determining step in the reaction of dioxygen with the copper(I) complexes shown in Scheme 1, or with directly related complexes, is the attack of dioxygen on copper(I). Unfortunately the kinetic findings do not reveal any information on the reaction steps following the binding of dioxygen, but this was also the case for the intramolecular ligand hydroxylation during the reaction of [Cu<sub>2</sub>(XYL-H)]<sup>2+</sup> with dioxygen (Figure 1).<sup>5</sup>

Our investigation of the reaction of dioxygen with the nitro derivative **2** did show very similar results to those found for **1**. No reversible formation of a peroxo complex could be observed, as Feringa and co-workers had claimed for **2** but without giving further details.<sup>27</sup> The rate constants were very close to those found for the reaction of **1** with dioxygen at 25 °C; no peroxo

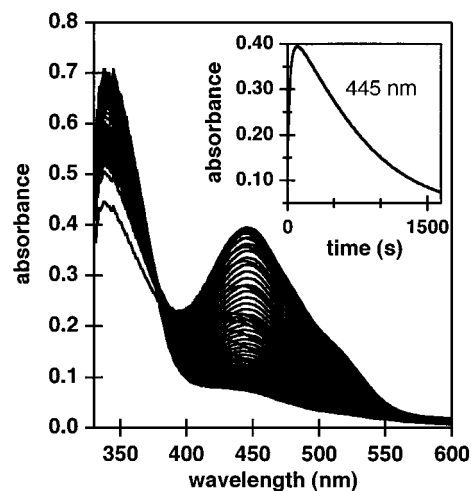


**Figure 7.** Spectral changes during the reaction of **2** with dioxygen in acetone in the presence of ~5% water ( $T = 25.0$  °C, [complex] = 0.18 mM, [O<sub>2</sub>] = 0.5106 mM).

complex was observed at low temperatures either. An important finding in that regard was that we observed the growth and disappearance of a band at 450 nm if water was present in the solution and no copper salt was used in excess (Figure 7). This band appearance again can be almost completely suppressed if [Cu(CH<sub>3</sub>CN)<sub>4</sub>](BF<sub>4</sub>) is added in excess. This makes it clear that this reaction arises from the right-hand side of the equilibrium in eq 2 and has nothing to do with the reaction of the dinuclear species with dioxygen, the reaction we are really interested in. Adding water to a solution of **1** also showed an effect, but this was very small compared to **2** (it also was suppressed by adding [Cu(CH<sub>3</sub>CN)<sub>4</sub>](BF<sub>4</sub>)). While the reaction is interesting, it is very difficult to exactly assign this band mostly because we do not know precisely the nature of the complex which reacts with dioxygen in that way.

## Conclusions

Our detailed kinetic study provided further insight into the intramolecular ligand hydroxylation reaction during the oxidation of copper(I) Schiff base complexes with dioxygen. Even though the reaction of dioxygen with **1** was accompanied by a number of side reactions, in contrast to an earlier study on a macrocyclic dinuclear copper(I) imine complex, we were able to obtain the activation parameters for this reaction and a possible mechanism is postulated. The kinetic findings support the occurrence of a peroxo complex as an intermediate, but this species cannot be detected spectroscopically.

**Acknowledgment.** The authors gratefully acknowledge financial support from the Deutsche Forschungsgemeinschaft, the Volkswagen-Stiftung, the British Council, and the DAAD. Furthermore, we thank Prof. Rudi van Eldik for valuable discussions.

**Supporting Information Available:** Listings of atomic coordinates and  $U$  values, bond distances and angles, anisotropic thermal parameters for non-hydrogen atoms, and hydrogen coordinates (10 pages). Ordering information is given on any current masthead page.

(34) Van Eldik, R.; Asano, T.; Le Noble, W. J. *Chem. Rev.* **1989**, *89*, 549.